Early detection of molecular disease progression by whole-genome circulating tumor DNA in advanced solid tumors

Andrew A. Davis[1,2], Wade T. Iams[3], David Chan[4], Michael S. Oh[1], Robert W. Lentz[1], Neil Peterman[5], Alex Robertson[4], Abhik Shah[5], Rohith Srivas[5], Nicole Lambert[5], Peter George[5], Becky Wong[5], Haleigh Wood[5], Jason Close[5], Ayse Tezcan[5], Ken Nesmith[5], Haluk Tezcan[5#], Young Kwang Chae[1,2#]

[1]Feinberg School of Medicine, Northwestern University, Chicago, IL
[2]Robert H. Lurie Comprehensive Cancer Center of Northwestern University, Chicago, IL
[3]Vanderbilt University Medical Center, Nashville, TN
[4]Cancer Care Associates TMPN, Redondo Beach, CA
[5]Lexent Bio, Inc., San Francisco & San Diego, CA
[#]corresponding authors: Haluk Tezcan: htezcan@lexentbio.com, Young Kwang Chae: ychae@nm.org

Notes about the manuscript

Funding statement: This study was supported by Lexent Bio, Inc.

Disclosures statement: **AAD** - travel support (Menarini Silicon Biosystems). **WTI** - advisory board (Genentech), honoraria (Outcomes Insights), investigator meeting (EMD Serono). **NP, AR, AS, RS, NL, PG, BW, HW, JC, AT, KN, & HT** - employees of and ownership interest in Lexent Bio. **AR, AS, KN, & HT** - previous employees of and ownership interest in Counsyl. **NL** - previous employee of and ownership interest in Sequenom. **PG** - previous employee of and ownership interest in Hologic. **YKC** - research grant (Abbvie, BMS, Biodesix, Lexent Bio, Freenome), honoraria/advisory board (Roche/Genentech, AstraZeneca, Foundation Medicine, Counsyl, Neogenomics, Guardant Health, Boehringher Ingelheim, Biodesix, Immuneoncia, Lilly Oncology, Merck, Takeda). **DC, MSO, & RWL** - none.

Abstract

Purpose: Treatment response assessment for patients with advanced solid tumors is complex and existing methods of assessment require greater precision for early disease assessment. Current guidelines rely on imaging, which has limitations such as the long time required before treatment effectiveness can be determined. Serial changes in whole-genome (WG) circulating tumor DNA (ctDNA) were used to detect disease progression early in the treatment course.

Methods: 97 patients with advanced cancer were enrolled, and blood was collected before and after initiation of a new treatment. Plasma cell-free DNA libraries were prepared for either WG or WG bisulfite sequencing. Longitudinal changes in the fraction of ctDNA were quantified to identify molecular progression or response in a binary manner. Study endpoints were agreement with first follow-up imaging (FUI) and stratification of progression-free survival (PFS).

Results: Patients with early molecular progression had shorter PFS (n=14; median 62d) compared to others (n=78; median 263d, HR 12.6 [95% confidence interval 5.8-27.3], log-rank $P<10^{-10}$, 5 excluded from analysis). All cases with molecular progression were confirmed by FUI and molecular progression preceded FUI by a median of 40d. Sensitivity for the assay in identifying clinical progression was 54%, median 24d into treatment and specificity was 100%.

Conclusions: Molecular progression, based on ctDNA data, detected disease progression for cases on treatment with high specificity approximately 6 weeks before follow-up imaging. This technology may enable early course change to a potentially effective therapy, avoiding side effects and cost associated with cycles of ineffective treatment.

Translational Relevance

Tools for early assessment of treatment response in advanced solid tumors require refinement. We performed baseline and early serial assessments of WG ctDNA to predict treatment response prior to standard of care clinical and radiographic assessments. Our results demonstrated that the blood-based prediction reliably identified molecular progression, approximately 6 weeks before imaging, with very high specificity and positive predictive value across multiple tumor and treatment types. Patients with molecular progression had significantly shorter progression-free survival compared with non-progressors. In addition, a large quantitative decrease in tumor fraction ratio was associated with significant durable benefit. Collectively, these findings demonstrate that cancer-related changes in the blood precede clinical or imaging changes and may inform changes in management earlier in the treatment course to improve long-term patient outcomes and limit cost.

Introduction

The current standard of care for evaluation of treatment response for advanced solid tumors is based on physical exam, patient reported symptoms, and periodic radiographic tumor assessment. However, there are limitations to these approaches as subtle changes in disease are often asymptomatic, and there are considerable costs, uncertainty, and anxiety associated with frequent imaging. In clinical trials, response criteria are standardized (e.g., RECIST, irRECIST) to guide evaluation by comparing a baseline scan before treatment initiation with periodic follow-up imaging (FUI) with pre-specified criteria for response. These criteria can be limited by the reliability of measurements over time, difficult to measure sites of disease (e.g., bone or pleural effusions), and challenges distinguishing pseudoprogression from true progression (1–3). Therefore, novel methods for monitoring response to treatment are needed given the emergence of new treatment modalities with ongoing questions regarding how best to manage treatment, minimize toxicity, and control cost. Here, we evaluated a blood-based approach using dynamic changes in WG ctDNA for early assessment of treatment response.

Liquid biopsy assays may analyze circulating cell-free DNA (cfDNA), circulating tumor cells (CTCs), RNA, exosomes, or proteins (4,5). ctDNA likely originates from cancer cells undergoing apoptosis, necrosis, or potential active mechanisms involving nucleic acid secretion to facilitate metastasis and gene expression at distant sites (6). The amount of ctDNA correlates with higher stages of disease and is also affected by tumor type, origin, location of metastasis, and treatment (7,8). There are several distinguishing features between ctDNA and non-tumor cfDNA. Specifically, as compared with cfDNA, ctDNA contains tumor-specific somatic point mutations, structural variations, shorter fragment lengths, biased fragment start and end positions, and changes in epigenetic patterns (9–16).

Copy number aberrations (CNA), which consist of either deletions or duplications of portions of the genome, are a common form of structural variation that are observed in patients with advanced disease at various sites across the genome (17). Prior studies have demonstrated that CNAs can be detected in cfDNA from patients by low-pass next-generation sequencing (NGS) with CNAs detected at a higher rate in patients with advanced disease (18). To date, changes in CNAs over time in advanced cancer patients remain understudied.

Recently, there has been significant interest in evaluating the potential clinical utility of ctDNA in advanced solid tumors. Prior work has demonstrated the prognostic value of ctDNA genomic alterations and mutant allele frequency as surrogates for tumor burden (19). In the adjuvant setting, residual ctDNA after surgery (e.g., minimal residual disease) has been associated with disease recurrence across multiple tumor types (8,20–23). In advanced disease, the most well validated clinical use is to identify driver mutations with known drug targets (24–27). Additionally, resistance mutations have been identified in the blood, guiding clinical management (28). While a few studies have evaluated the potential role of ctDNA for tumor response assessment in melanoma, non-small cell lung cancer, breast cancer, and prostate cancer,

among other tumor types, the clinical utility for routine assessment has not yet been established (8,29–36).

Here, in a prospectively enrolled, advanced stage, pan-cancer cohort, we performed whole-genome cfDNA analysis as a molecular marker of disease progression earlier in the treatment course compared with routine clinical and radiographic assessment of disease. In contrast to analyzing particular genes, our approach utilized CNAs and fragmentation patterns across the genome, a technique with broad potential clinical applications across multiple tumor types. Furthermore, for a subset of patients, we performed bisulfite conversion as part of the assay, which provided insight into genome-wide methylation changes. We hypothesized that early changes in cancer-associated signals in the blood would be predictive of response status at the time of first FUI and that the magnitude of the dynamic change in signal would provide longer-term prognostic information across a variety of solid tumor types and treatments.

Patients and Methods

Study subjects

The study sample here represented a subset of a currently accruing longitudinal observational study. From May 2017 to December 2018, participants (age >18 years) were prospectively enrolled from five oncology centers in the USA (TMPN - Cancer Care, Redondo Beach, CA; Scripps - California Cancer Associates, San Diego, CA; Sharp Memorial Hospital, San Diego, CA; Summit Cancer Centers, Post Falls, ID; Robert H. Lurie Comprehensive Cancer Center of Northwestern University, Chicago, IL) and followed through June 2019 (Table 1). Eligibility criteria were:

- Diagnosis of a non-hematologic and surgically unresectable advanced tumor (stage III or higher) at presentation
- Commencement of a new systemic treatment regimen of the physician's choice
- Presence of either measurable or evaluable disease by imaging

To be included in this cohort, the participants needed to have venous blood samples from at least two time points: a baseline (T0, before treatment initiation) and another one before cycle 2 (T1) and/or cycle 3 (T2, Fig. 1A). This study was conducted in accordance with the Declaration of Helsinki and approved by Northwestern University, Sharp Memorial Hospital and Western Institutional Review Boards. An informed consent was obtained from each patient prior to participation in the study.

Evaluation of response status

Participants were radiologically assessed at baseline and again at first follow-up as determined per standard of care routine clinical assessment. The primary endpoint of the study was evidence of radiographic progression as determined by Response Evaluation Criteria in Solid Tumors (RECIST) version 1.1 (37) or clinical response evaluation. Measurable disease by imaging was

interpreted by the treating physician facility and an independent radiologist, who was blinded to the assessment of molecular response. When RECIST outcome could not be ascertained due to either non-evaluable or missing imaging study, clinical response evaluation was used. Clinical response was defined as the physician's outcome assessment before a treatment change and was categorized as clinical progressive disease (PD), responsive disease (nonPD), stable disease (nonPD), or too early to assess.

PFS was defined as the time from the start of treatment to first documentation of PD, or death due to any cause, whichever occurred first. Patients last known to be alive and progression-free were censored at the date of last contact. Patients were considered as lost-to-follow-up if they were no longer part of the study and their status was unknown (non-assessable case).

Sample preparation

At each time point, 10 mL of whole blood was collected in Streck Cell-Free DNA BCT. Plasma was separated via centrifugation at 1600 x g for 15 minutes followed by 2500 x g for 10 minutes within 7 days from the time of collection. cfDNA was extracted from plasma using the Qiagen QIAmp MinElute ccfDNA kit and stored at -80C until library preparation. For each patient, libraries were prepared using the KAPA HyperPrep library prep kit for whole genome sequencing (WGS; n=54 patients) or the Nugen Ovation Ultralow Methyl-Seq whole genome bisulfite sequencing kit (WGBS; n=43 patients). Average input cfDNA into the library preparation was 20 ng. Libraries were sequenced on the Illumina HiSeq X to an average depth of 20X (range 6-29X).

Bioinformatics methods

Tumor fraction ratio (TFR) was measured to assess changes in ctDNA using CNAs and local changes in cfDNA fragment length, both assessed from sequencing data. Reads were aligned to the human genome (GRCh37) with a custom bioinformatics pipeline based on BWA (38), sambamba (39), and samtools (40). Reads were then de-duplicated and GC biases were corrected using the deepTools software package (41). CNAs were detected using a pipeline based on ichorCNA (18) and custom algorithms. Normalized fragment length was computed by normalizing by library and genomic location. Background signals for CNA and fragment length were established for each sequencing protocol using healthy normal samples taken from 44 individuals with no current or prior diagnosis of any malignancy (Supp. Table S1). In order to maximize sensitivity of CNAs while preventing false positive detections, Spearman's rank correlation between local mean fragment length and copy number was used as a disqualifier of CNA call sets (42,43).

To assess changes in ctDNA over time, direct comparison of the CNA-derived estimate of TF between a patient's time points was not always reliable because there was ambiguity in which read depth levels correspond to which structural events. For example, two regions might be called as either a neutral region and a duplicated region, or a heterozygous deletion and a neutral

region, in a highly mutated tumor where there was an ambiguous neutral level. To circumvent this, CNAs detected at multiple time points were compared longitudinally with a linear model to quantify TFR. In order to determine confident calls, measured changes were compared to a simulated background model and required to exceed a Z-score threshold of 3. No longitudinal comparisons of samples from 44 healthy participants (Supp. Table S1) showed a significant change in TFR (e.g. Supp. Fig. S1). Cases that showed a confident increase in tumor fraction indicated by TFR greater than 1 at either time point were classified as molecular progression. Major molecular response (MMR) was defined as TFR < 0.1.

Statistical Analysis

For the purposes of calculating sensitivity, specificity, positive predictive value and negative predictive value, true positives were defined as cases where the assay showed a molecular progression which were also evaluated as PD either clinically or by RECIST 1.1 at first FUI; true negatives were cases where both the assay and clinical evaluation did not call PD at first follow-up. False positives and false negatives were cases where molecular response assessment disagreed with the first FUI with either a clinical or radiographic progression or lack of a clinical or radiographic progression respectively. Confidence intervals on these metrics were computed with the Wilson's score interval method.

Survival curves were generated using the Kaplan-Meier method and differences in PFS between molecular progressors and non-progressors assessed using the log-rank test. The Cox proportional hazards model was used for the assessment of the effects of different magnitudes of change on PFS. Statistical analyses of survival were performed with the R survival package version 2.41-3 and other statistical analyses were determined using the python scipy package version 1.1.0.

Results

Patient characteristics

A total of 97 patients with advanced cancer, who fit the inclusion criteria of the study and had appropriate long-term follow-up data, were sequenced for the analysis. Baseline blood samples failed sequencing for five participants, therefore they were excluded. The remaining 92 patients with NGS and clinical outcome data were included in this analysis. The median age was 70 years and 55% were females (Table 1). About half of the participants received a first-line therapy (52%) and 25% received a second-line therapy. The majority of patients had lung cancer (44%) or breast cancer (27%) with the remainder representing gastrointestinal cancers (15%), genitourinary cancers (6.5%), melanoma (6.5%) and sarcoma (1%). During the study, 46% of all participants received chemotherapy (+/- antibody treatment) and 37% received immunotherapy with or without chemotherapy (n=34, Table 1, Supp. Table S2). The first FUI occurred a median of 71 days after treatment start (Fig. 1B, min=26 days, max=208 days). Three participants

received an outcome assignment based on clinical evaluation. Of these 3 participants, one had a non-evaluable imaging study and was assessed as clinical nonPD at week-12, and two did not have an imaging study prior to treatment change, and these patients were assessed as clinical PD at week-9 and week-19 by the treating physician. The median follow-up time of the full cohort was 140 days (min=35 days, max=645 days).

Baseline blood samples were collected prior to treatment start for all patients (Fig. 1B, median=0 days after treatment start, min=−19 days). One or two post-treatment samples were collected for each patient, with T1 collected prior to the second cycle of therapy at a median of 21 days after treatment start (n=86, min=9 days, max=40 days) and T2 collected prior to the third cycle of therapy at a median of 42 days (n=66, min=37 days, max=84 days). Both post-treatment samples were collected for 60 patients.

Serial measurements of ctDNA showed rapid changes early on treatment

We assessed changes in tumor fraction using WG analysis to quantify the TFR between baseline and post-treatment samples. Substantial changes in TFR were observed early after treatment initiation (Fig. 2). Patient LS030178 demonstrated an example of a rapid increase in TFR to 2.4 at T1 following the first cycle of therapy, indicating a major increase from baseline, followed by an even greater increase at T2 (Fig. 2A-D). This patient had a somatic gain of the long arm of chromosome 1 (1q), which has been shown to be one of the most common arm-level aberrations in breast cancer (44). Additionally, the strong pattern of CNAs was corroborated by the fragmentation pattern (Fig. 2B-C). Conversely, patient LS030093 showed a decrease in TFR at T1 and then a larger decrease at T2 (Fig. 2E).

A subset of samples had both WGS and WGBS and were used to test whether TFR could be quantified equivalently across sequencing protocols (Supp. Fig. S2). TFR values were highly concordant between WGS and WGBS, enabling analysis of the full cohort including samples analyzed with both protocols.

Tracking changes in tumor fraction at early time points predicted progression at first follow-up response assessment

At the first FUI and clinical evaluation, 26 of 92 patients had clinical PD and 66 had nonPD. To evaluate the predictive value of the ctDNA assay, we compared the classification of molecular progression to clinical assessment at first FUI for all patients (Fig. 3A). All 14 patients with a molecular progression at either T1 or T2 had PD, and likewise of the 66 patients who were nonPD, none had molecular progression. The sensitivity of the assay including time points T1 and T2 was 54% and specificity was 100%. The sensitivity was 42% at T1 and was 61% at T2 (Fig. 3B). There was no statistically significant relationship between sensitivity and timing of the blood draw (Supp. Fig. S3). In the cases where molecular progression was called, the time point where it was first identified preceded the detection of progression by imaging by a median of 40 days (Fig. 3C).

Among the 12 patients with PD at first FUI where there was a discrepancy between imaging and molecular assessment of progression, 3 had no confident CNAs detected, 2 had no significant change in tumor fraction, and 7 had a decrease in tumor fraction. For the discordant cases with a decrease in tumor fraction, there were a variety of cancer types represented (3 breast, 2 lung, 1 renal, 1 sarcoma), treatments (4 chemotherapy, 1 immunotherapy, 1 endocrine therapy, 1 targeted therapy alone), and lines of therapy (3 first, 2 second, 1 third, 1 fifth). Additionally, there were no major difference in predictive performance between WGS and WGBS (Supp. Table S3).

Molecular response pattern assessed by cfDNA early on treatment was correlated with PFS

The median PFS for the full cohort of patients was 211 days (Fig. 4A). Patients with molecular progression at either T1 or T2 (n=14) had shorter PFS, with HR 12.6 (95% CI 5.8-27.3; Log-rank $P=7\times10^{-16}$) and median PFS of 63 days vs. 263 days for patients with no molecular progression (n=78; Fig. 4B).

The predictive performance of the assay was explored in subsets of patients based on tumor origin and treatment type. Among the 34 patients who received immunotherapy, PFS was significantly shorter in patients with molecular progression (median PFS=57 days) compared to patients without identified molecular progression (median PFS not reached after a median of 167 days follow-up, log-rank $P=2\times10^{-12}$), consistent with the overall cohort (Fig. 4C). The results were similar for the chemotherapy subset with a median PFS of 56 days in patients with molecular progression and 212 days without progression (Fig. 4D; n=42; log-rank $P=7\times10^{-6}$). PFS was also significantly shorter for patients with molecular progression for the two largest subsets, lung cancer (Fig. 4E; log-rank $P=8\times10^{-8}$) and breast cancer (Fig. 4F; log-rank $P=3\times10^{-4}$). This was also true for the remaining subset of mixed cancer types (gastrointestinal, genitourinary, melanoma, and sarcoma, Supp. Fig. S4; log-rank $P=5\times10^{-6}$). Predictions of progression at first FUI also had comparable performance across these subsets (Supp. Table S4). Together, these data suggest that the assay was effective across multiple cancer types and treatment modalities.

We explored whether a large quantitative reduction early in the treatment course was associated with an improved PFS. Of the 78 patients for whom the assay did not show molecular progression, 27 had an MMR at either post-treatment time point. Notably, in all cases where a MMR was identified at T1, this finding was also observed at T2, if that time point was available (n=12). In 7 cases the TFR from baseline did not reach a 10-fold reduction at T1 but did at T2, for example for patient LS030093 (Fig. 2E). Patients with an MMR had longer PFS (Fig. 4G, median PFS not reached) compared to patients with no MMR and no molecular progression (n=51; median PFS of 211 days). A MMR was significantly predictive of PFS after accounting for the predictions based on molecular progression (Stratified Cox: molecular progression $P=4\times10^{-9}$, MMR P=0.011), indicating value in the early quantitative ctDNA dynamics for predicting longer term treatment efficacy.

Next, we sought to assess the predictive value of an MMR in conjunction with radiographic response monitoring. For patients who did not show radiographic progression at first FUI (n=65), RECIST 1.1 based partial response vs. stable disease at first FUI had limited prognostic value for PFS (Fig. 4H; log-rank P=0.4; HR 0.67 [95% CI 0.28-1.60]). However, among the same subset, patients with an MMR had substantially longer PFS (Fig. 4I; log-rank P=0.02; HR 0.28 [95% CI 0.09-0.84]), which was also significant after adjusting for radiographic assessment at first FUI (Stratified Cox: partial response P=0.36, MMR P=0.016; Supp. Fig. S5).

Longitudinal changes in methylation levels may complement tumor fraction changes

Global hypomethylation is a hallmark of tumor genomes (17, 48), and an increase in global methylation levels in cfDNA might be associated with non-progression as it would indicate a decreased proportion of ctDNA. Importantly, the epigenetic patterns observed in tumors, including overall global hypomethylation can be detected in ctDNA (45,46). To assess the potential of methylation changes for identifying early response to therapy, the change in genome-wide methylation levels from baseline to post-treatment was examined retrospectively for two example patients (Figure 5)—one with a nonPD call (LS030083) at first FUI and one with a PD call at first FUI (LS030078). Consistent with the clinical assessment at first FUI, a marked increase in methylation levels was observed for LS030083 (Figure 5A), while a decrease was observed in LS030078 (Figure 5B). For patient LS030078, a clear molecular progression was observed based on CNAs and local fragmentation changes (TFR=2.01), while no CNAs were detectable in LS030083.

Discussion

Patients with advanced malignancies require careful treatment monitoring to assess therapeutic efficacy, promote quality of life, and limit drug toxicity. Current methods for disease monitoring using clinical and radiographic assessment often require several months to confidently determine treatment response. Here, we assessed the utility of a novel, whole-genome cfDNA molecular response assay, which analyzed longitudinal ctDNA measurements at baseline and during the initial cycles of treatment to predict response to therapy. This technique predicted disease progression with both a specificity and PPV of 100%, indicating that when this assay predicted disease progression, there was high confidence and reliability at a median of 6 weeks before current standard of care methods. This finding indicates that advanced tumors that are progressing early in the course of treatment are declaring this in the blood well before visible change in the size, contour, or density of target lesions that can be detected by current imaging schedule and interpretation.

Our study has several other key findings. First, the blood-based, whole-genome ctDNA molecular assay appeared to predict disease progression consistently across a variety of tumor

and treatment types, by looking beyond targeted assessment of tumor-specific point mutations and fusions. Specifically, subset analyses of the two cohorts with the largest number of patients (lung and breast cancer) demonstrated statistically significant findings, which were also observed collectively across non-lung and non-breast patients. Similar predictive value was encountered across different treatments, including patients who received chemotherapy or immunotherapy. These findings build on previous work that also utilized a CNA-based approach for a cohort of patients treated with immunotherapy alone (47). Second, we demonstrated that patients with an MMR had a longer PFS compared to those with no change or a smaller decrease in TFR, indicating that there was quantitative value in the degree of initial response to therapy. In our data, PFS was more strongly associated with the degree of response measured by the assay, as compared with RECIST 1.1 classification of partial response vs. stable disease, indicating that radiographic assessment of partial response vs. stable at first FUI may have limited long-term prognostic value in some cases. The additional prognostic value of identifying an MMR supports the potential to integrate imaging and analysis of serial cfDNA samples to provide an early indication of an extended duration of disease control.

Molecular response monitoring with serial measurements of cfDNA has potential clinical benefit for both assessing disease control and disease progression. For example, if MMR is observed, early reassurance that the current treatment regimen is effective could limit frequency of imaging, if our findings are validated in larger cohorts. In contrast, an early prediction of blood-based molecular progression could guide oncologists to discontinue ineffective treatments, thereby reducing avoidable side effects and financial toxicity. By accelerating the clinical decision loop, patients would be afforded the opportunity to change to an alternative, potentially effective therapy. This assessment algorithm may increase the availability of patients with adequate performance status to engage in multiple lines of therapy, including clinical trials. Furthermore, a blood-based assay provides convenience for patients as blood samples are collected routinely during each cycle of therapy.

This study has several limitations. First, while the specificity of the assay was very high, which is the critical performance metric for clinical utility in the advanced setting, sensitivity was relatively low. Sensitivity, particularly at the earliest time point, may be improved by including other features such as cancer-associated epigenetic signals. For example, in patient LS030083, there was a marked increase in genome-wide methylation levels from baseline to post-treatment, consistent with a nonPD call at first FUI, yet no CNAs were detected (Figure 5A). In future work, we plan to incorporate these methylation-based signals into the assay, along with fragment length and copy number information to increase assay sensitivity. However, even with additional orthogonal signals, there will likely be a residual false negative rate from a) tumors that do not generate sufficient ctDNA (e.g., non-shedding tumors), b) tumors that have not yet progressed during the earliest cycles of treatment and, c) tumors in which molecular progression by ctDNA analysis and imaging are not in agreement. Second, expanded patient cohorts are required to confirm the tumor and treatment-agnostic nature of the assay. Third, prospective validation of the prediction tool is needed. Future studies will examine an independent validation cohort and assess how treatment changes using an adaptive clinical trial design may both limit cost and improve long-term patient outcomes by switching to different treatment arms faster using the blood-based molecular response assessment.

In conclusion, we demonstrated that a serial monitoring approach analyzing whole-genome ctDNA with low-pass sequencing produced clinical predictions with a high degree of specificity and PPV compared with standard of care clinical assessment. In addition, the findings were consistent across multiple tumor and treatment types, and the degree of ctDNA reduction appeared to correlate with long-term clinical outcome. If validated prospectively, this non-invasive tool may more accurately match advanced cancer patients with potentially effective therapies earlier and limit side effects and costs associated with ineffective treatments.

Acknowledgements

We thank all participants and their families for participating in this study. We also thank Dr. Brian McNamee for review of all clinical images, as well as all clinicians and their research staff.

Figures and Table

	Median (Min-Max)	N= 92 (%)
Age	70 (30-89)	
Sex		
Female		51 (55.4)
Male		41 (44.6)
Cancer type		
Lung		40 (43.5)
Breast		25 (27.2)
GI		14 (15.2)
GU		6 (6.5)
Melanoma		6 (6.5)
Sarcoma		1 (1.1)
Treatment types		
Chemotherapy		32 (34.8)
Chemotherapy, Antibody		10 (10.9)
Immunotherapy		25 (27.2)
Immunotherapy, Chemotherapy		9 (9.8)
Endocrine		3 (3.3)
Endocrine, CDK4/6i		7 (7.6)
Targeted alone		6 (6.5)
Lines of therapy		
1		48 (52.2)
2		23 (25.0)
3+		21 (22.8)
T1 (days)	21 (9-40)	86 (93.5)
T2 (days)*	42 (37-84)	66 (71.7)
First follow-up (days)	71 (26-208)	
Last follow-up (days)	140 (35-645)	

* 60 participants had both post-treatment time points

Table 1. Participant characteristics. Distribution of blood sample and follow-up times are with respect to on-study treatment times, May 2017 - June 2019.

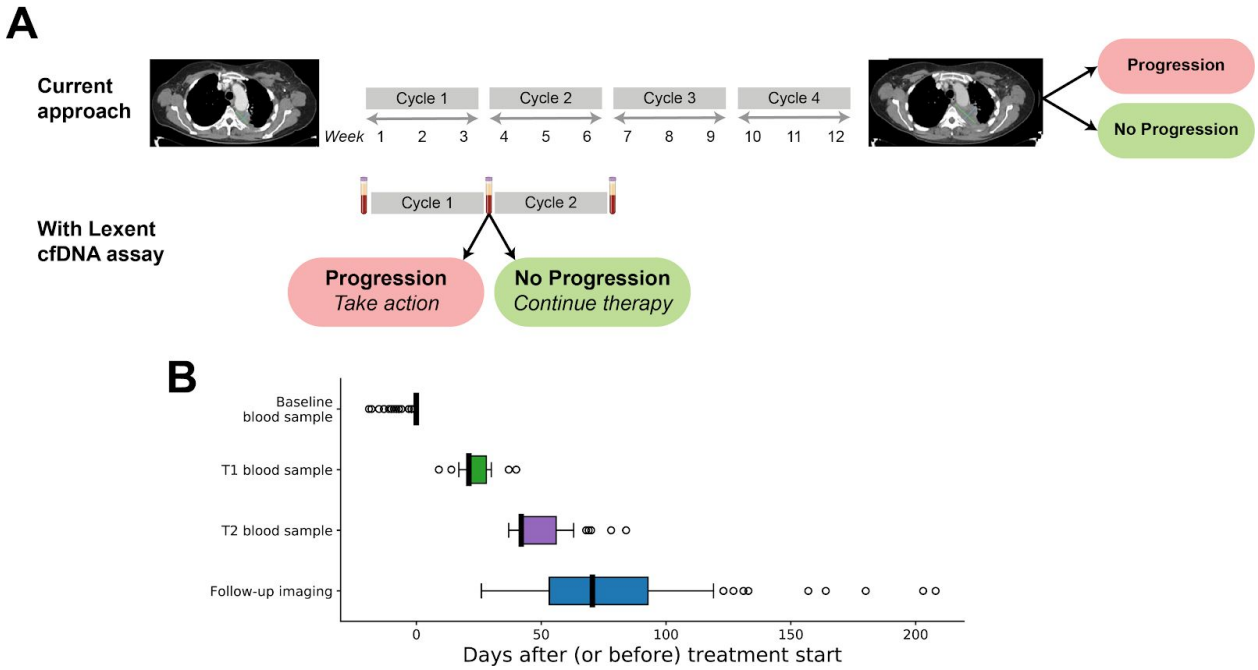

Figure 1. Overview of the clinical setting. A. Diagram comparing radiographic response assessment and the potential use of cfDNA to assess molecular response**. B.** Timing of imaging and blood collections for patients in the study.

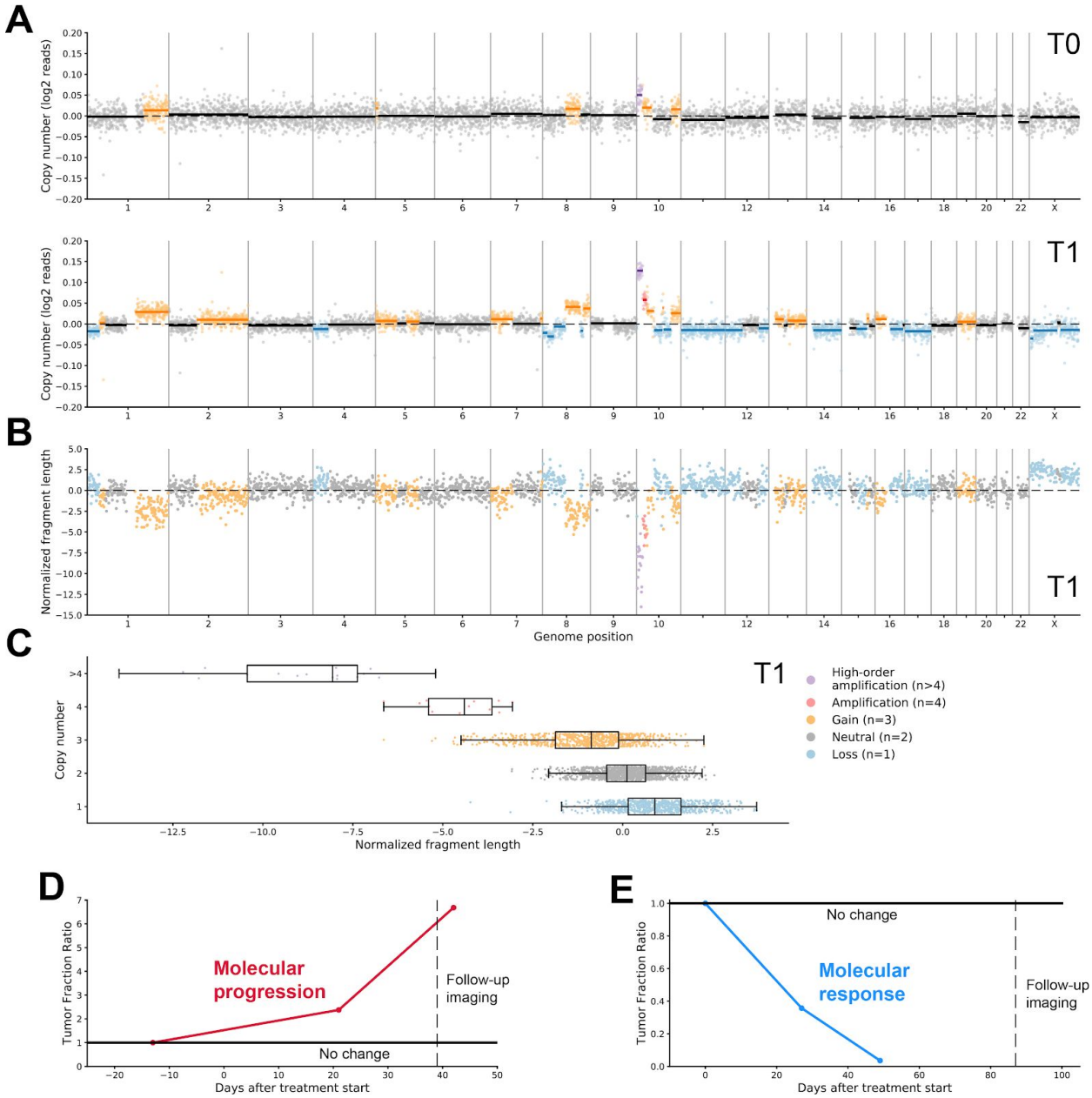

Figure 2. Serial assessment of ctDNA to determine molecular progression. A. The genome-wide plots of CNAs detected for patient LS030178. The T0 baseline blood draw was collected 13 days before the start of treatment, and T1 was collected 21 days after the start of treatment. **B.** Normalized fragment length exhibit the reverse pattern compared to CNAs. **C.** Overall there was a strong negative correlation between the normalized fragment length at each genomic position and the inferred copy number (Spearman's rho=-0.57, $P<10^{-10}$). **D.** Patient LS030178 had an increase in TFR at follow-up time points T1 and T2, detectable in advance of imaging that indicated progressive disease. **E.** Patient LS030093, who responded to therapy, showed a marked decrease in TFR at T1 and T2, concordant with later imaging that showed a partial response.

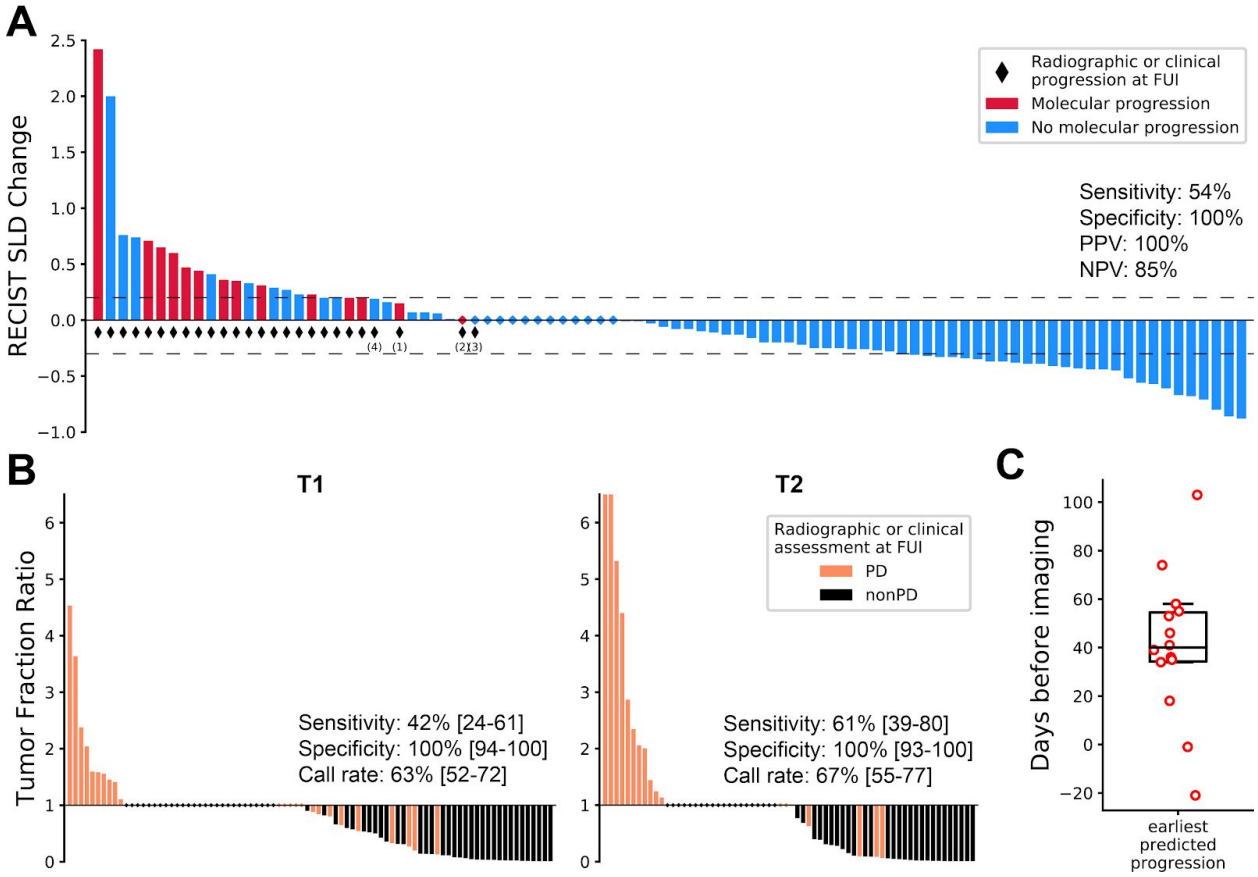

Figure 3. ctDNA assessments following first or second cycle of therapy predicted progression. A. Comparison of imaging results at first FUI (SLD assessed by RECIST 1.1) with ctDNA assessment of molecular progression, indicated by a confident increase in TFR for either post-treatment sample (sensitivity=54%, specificity=100%, PPV=100%, NPV=85%). Footnoted cases showed clear clinical progression. **B.** TFR for progressors and non-progressors at T1 (left) and T2 (right), compared to radiographic or clinical assessment of PD or nonPD, showing predictive performance at each time point. **C.** For patients with molecular progression, detection of the molecular progression preceded the date of detection of progression by standard of care imaging by a median of 40 days (range -21 to 103).

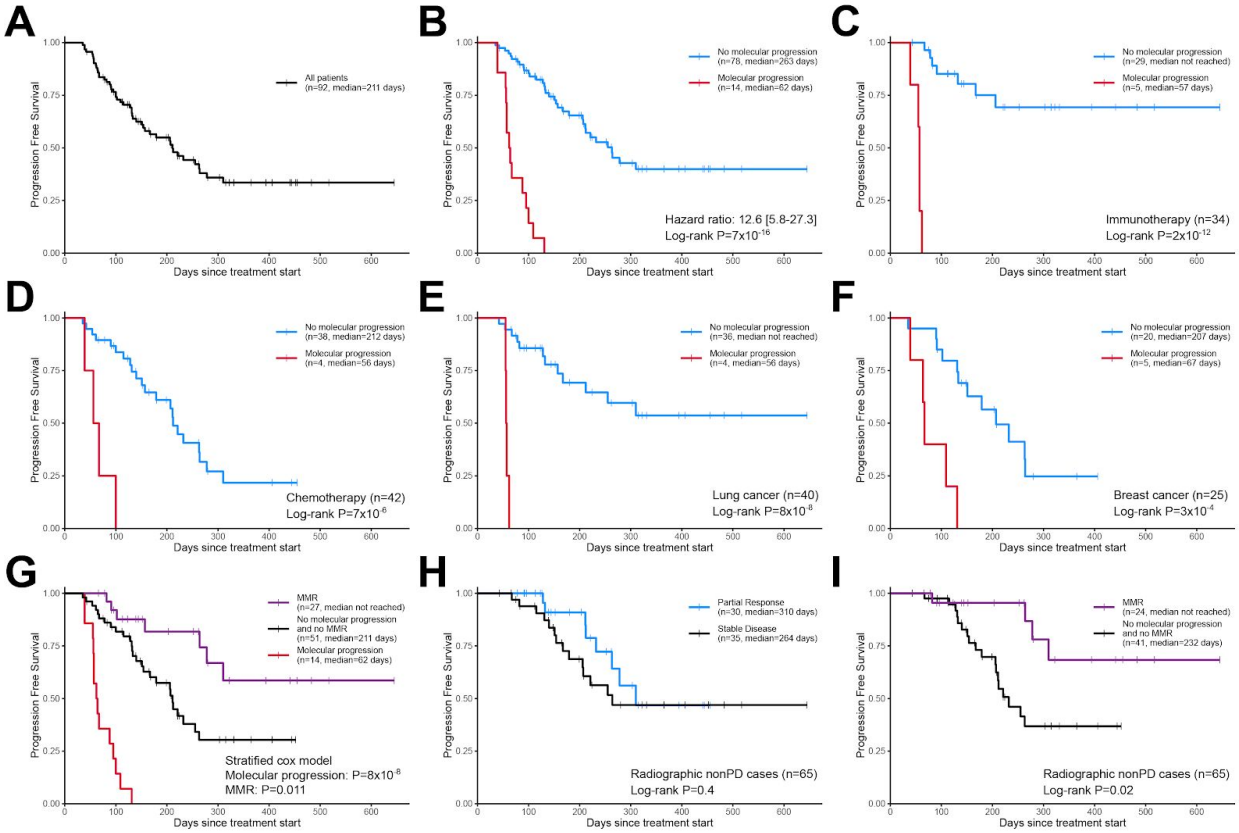

Figure 4. Molecular response assessment early in the course of therapy was associated with favorable PFS. A. The full cohort (n=92) had median PFS of 211 days. **B.** Patients with a molecular progression detected from cfDNA at T1 or T2 (n=14, median PFS=62 days) had significantly worse PFS compared to patients with no molecular progression (n=78, median PFS=263 days; HR=12.6 [5.8-27.3]; log-rank $P<10^{-10}$). **C-D.** Subset analysis based on therapeutic modality for **(C)** patients on immunotherapy with or without chemotherapy (n=34; log-rank $P=2\times10^{-12}$), and **(D)** patients on chemotherapy with or without targeted therapy (n=42; log-rank $P=7\times10^{-6}$). **E-F.** Subset analysis based on cancer type for **(E)** Lung cancer patients (n=40; log-rank $P=8\times10^{-8}$) and **(F)** breast cancer patients (n=25; log-rank $P=3\times10^{-4}$). **G.** Patients with a MMR had significantly longer PFS after accounting for predictions based on molecular progression (Cox P=0.011). **H-I.** Subset analysis for patients with either stable disease or partial response determined by radiography at first FUI (n=65) stratified by **(H)** response status (log-rank P=0.4) or **(I)** MMR (log-rank P=0.02).

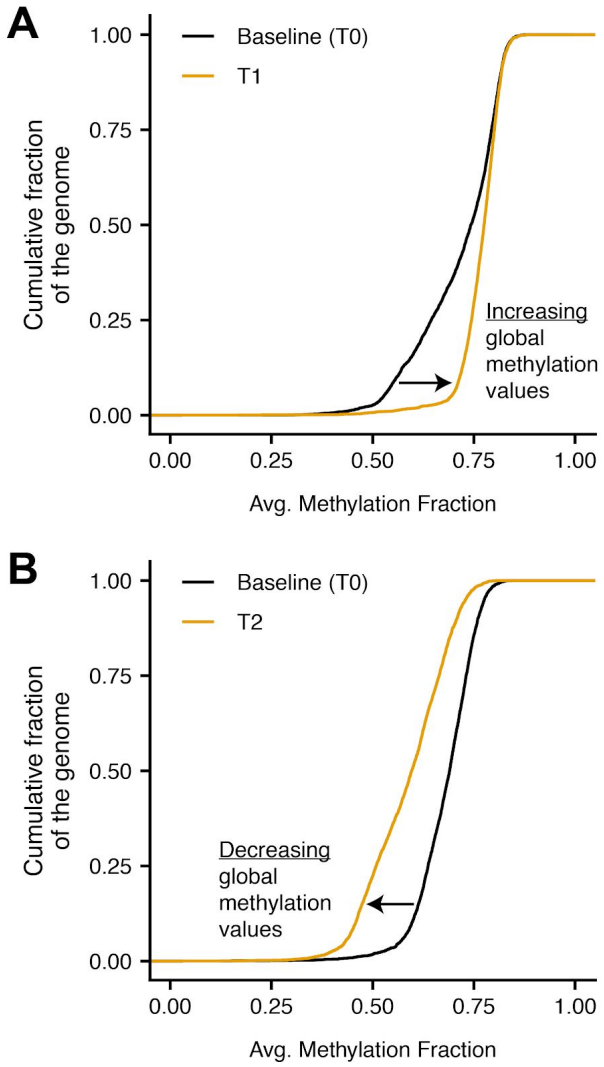

Figure 5. Methylation may provide an orthogonal signal to CNAs for response monitoring. A-B. Distribution of average methylation levels in genome-wide 1 megabase bins for patient **(A)** LS030083 and **(B)** LS030078 at baseline (black line) and either T1 or T2 (orange line).

References

1. Erasmus JJ, Gladish GW, Broemeling L, Sabloff BS, Truong MT, Herbst RS, et al. Interobserver and intraobserver variability in measurement of non-small-cell carcinoma lung lesions: implications for assessment of tumor response. J Clin Oncol. 2003;21:2574–82.
2. Nishino M, Giobbie-Hurder A, Manos MP, Bailey N, Buchbinder EI, Ott PA, et al. Immune-Related Tumor Response Dynamics in Melanoma Patients Treated with Pembrolizumab: Identifying Markers for Clinical Outcome and Treatment Decisions. Clin Cancer Res. 2017;23:4671–9.
3. Chiou VL, Burotto M. Pseudoprogression and Immune-Related Response in Solid Tumors. J Clin Oncol. 2015;33:3541–3.
4. Wan JCM, Massie C, Garcia-Corbacho J, Mouliere F, Brenton JD, Caldas C, et al. Liquid biopsies come of age: towards implementation of circulating tumour DNA. Nat Rev Cancer. 2017;17:223–38.
5. Siravegna G, Marsoni S, Siena S, Bardelli A. Integrating liquid biopsies into the management of cancer. Nat Rev Clin Oncol. 2017;14:531–48.
6. Heitzer E, Ulz P, Geigl JB. Circulating tumor DNA as a liquid biopsy for cancer. Clin Chem. 2015;61:112–23.
7. Chen K-Z, Lou F, Yang F, Zhang J-B, Ye H, Chen W, et al. Circulating Tumor DNA Detection in Early-Stage Non-Small Cell Lung Cancer Patients by Targeted Sequencing. Sci Rep. 2016;6:31985.
8. Merker JD, Oxnard GR, Compton C, Diehn M, Hurley P, Lazar AJ, et al. Circulating tumor DNA analysis in patients with cancer: american society of clinical oncology and college of american pathologists joint review. J Clin Oncol. 2018;36:1631–41.
9. Murtaza M, Dawson S-J, Tsui DWY, Gale D, Forshew T, Piskorz AM, et al. Non-invasive analysis of acquired resistance to cancer therapy by sequencing of plasma DNA. Nature. 2013;497:108–12.
10. Chan KCA, Jiang P, Zheng YWL, Liao GJW, Sun H, Wong J, et al. Cancer genome scanning in plasma: detection of tumor-associated copy number aberrations, single-nucleotide variants, and tumoral heterogeneity by massively parallel sequencing. Clin Chem. 2013;59:211–24.
11. Mouliere F, Robert B, Arnau Peyrotte E, Del Rio M, Ychou M, Molina F, et al. High fragmentation characterizes tumour-derived circulating DNA. PLoS ONE. 2011;6:e23418.
12. Jiang P, Chan CWM, Chan KCA, Cheng SH, Wong J, Wong VW-S, et al. Lengthening and shortening of plasma DNA in hepatocellular carcinoma patients. Proc Natl Acad Sci USA. 2015;112:E1317-25.
13. Underhill HR, Kitzman JO, Hellwig S, Welker NC, Daza R, Baker DN, et al. Fragment length of circulating tumor DNA. PLoS Genet. 2016;12:e1006162.
14. Snyder MW, Kircher M, Hill AJ, Daza RM, Shendure J. Cell-free DNA Comprises an In Vivo Nucleosome Footprint that Informs Its Tissues-Of-Origin. Cell. 2016;164:57–68.
15. Jiang P, Sun K, Tong YK, Cheng SH, Cheng THT, Heung MMS, et al. Preferred end coordinates and somatic variants as signatures of circulating tumor DNA associated with hepatocellular carcinoma. Proc Natl Acad Sci USA. 2018;115:E10925–33.
16. Sun K, Jiang P, Chan KCA, Wong J, Cheng YKY, Liang RHS, et al. Plasma DNA tissue mapping by genome-wide methylation sequencing for noninvasive prenatal, cancer, and transplantation assessments. Proc Natl Acad Sci USA. 2015;112:E5503-12.

17. Beroukhim R, Mermel CH, Porter D, Wei G, Raychaudhuri S, Donovan J, et al. The landscape of somatic copy-number alteration across human cancers. Nature. 2010;463:899–905.

18. Adalsteinsson VA, Ha G, Freeman SS, Choudhury AD, Stover DG, Parsons HA, et al. Scalable whole-exome sequencing of cell-free DNA reveals high concordance with metastatic tumors. Nat Commun. 2017;8:1324.

19. Schwaederlé MC, Patel SP, Husain H, Ikeda M, Lanman RB, Banks KC, et al. Utility of Genomic Assessment of Blood-Derived Circulating Tumor DNA (ctDNA) in Patients with Advanced Lung Adenocarcinoma. Clin Cancer Res. 2017;23:5101–11.

20. Pantel K, Alix-Panabières C. Liquid biopsy and minimal residual disease - latest advances and implications for cure. Nat Rev Clin Oncol. 2019;

21. Abbosh C, Birkbak NJ, Swanton C. Early stage NSCLC - challenges to implementing ctDNA-based screening and MRD detection. Nat Rev Clin Oncol. 2018;15:577–86.

22. Chae YK, Oh MS. Detection of Minimal Residual Disease Using ctDNA in Lung Cancer: Current Evidence and Future Directions. J Thorac Oncol. 2019;14:16–24.

23. Rossi G, Ignatiadis M. Promises and pitfalls of using liquid biopsy for precision medicine. Cancer Res. 2019;

24. Lanman RB, Mortimer SA, Zill OA, Sebisanovic D, Lopez R, Blau S, et al. Analytical and Clinical Validation of a Digital Sequencing Panel for Quantitative, Highly Accurate Evaluation of Cell-Free Circulating Tumor DNA. PLoS ONE. 2015;10:e0140712.

25. Diaz LA, Bardelli A. Liquid biopsies: genotyping circulating tumor DNA. J Clin Oncol. 2014;32:579–86.

26. Reckamp KL, Melnikova VO, Karlovich C, Sequist LV, Camidge DR, Wakelee H, et al. A highly sensitive and quantitative test platform for detection of NSCLC EGFR mutations in urine and plasma. J Thorac Oncol. 2016;11:1690–700.

27. Juric D, Ciruelos E, Rubovszky G, Campone M, Loibl S, Rugo HS, et al. Abstract GS3-08: Alpelisib + fulvestrant for advanced breast cancer: Subgroup analyses from the phase III SOLAR-1 trial. Cancer Res. 2019;79:GS3-08-GS3-08.

28. Fribbens C, O'Leary B, Kilburn L, Hrebien S, Garcia-Murillas I, Beaney M, et al. Plasma ESR1 Mutations and the Treatment of Estrogen Receptor-Positive Advanced Breast Cancer. J Clin Oncol. 2016;34:2961–8.

29. Xi L, Pham TH-T, Payabyab EC, Sherry RM, Rosenberg SA, Raffeld M. Circulating Tumor DNA as an Early Indicator of Response to T-cell Transfer Immunotherapy in Metastatic Melanoma. Clin Cancer Res. 2016;22:5480–6.

30. Lee JH, Long GV, Boyd S, Lo S, Menzies AM, Tembe V, et al. Circulating tumour DNA predicts response to anti-PD1 antibodies in metastatic melanoma. Ann Oncol. 2017;28:1130–6.

31. Váraljai R, Wistuba-Hamprecht K, Seremet T, Diaz JMS, Nsengimana J, Sucker A, et al. Application of Circulating Cell-Free Tumor DNA Profiles for Therapeutic Monitoring and Outcome Prediction in Genetically Heterogeneous Metastatic Melanoma. JCO Precis Oncol. 2019;1–10.

32. Pécuchet N, Zonta E, Didelot A, Combe P, Thibault C, Gibault L, et al. Base-Position Error Rate Analysis of Next-Generation Sequencing Applied to Circulating Tumor DNA in Non-Small Cell Lung Cancer: A Prospective Study. PLoS Med. 2016;13:e1002199.

33. Anagnostou V, Forde PM, White JR, Niknafs N, Hruban C, Naidoo J, et al. Dynamics of Tumor and Immune Responses during Immune Checkpoint Blockade in Non-Small Cell Lung Cancer. Cancer Res. 2019;79:1214–25.

34. Hrebien S, Citi V, Garcia-Murillas I, Cutts R, Fenwick K, Kozarewa I, et al. Early ctDNA dynamics as a

surrogate for progression free survival in advanced breast cancer in the BEECH trial. Ann Oncol. 2019;

35. Choudhury AD, Werner L, Francini E, Wei XX, Ha G, Freeman SS, et al. Tumor fraction in cell-free DNA as a biomarker in prostate cancer. JCI Insight. 2018;

36. Kurtz DM, Scherer F, Jin MC, Soo J, Craig AFM, Esfahani MS, et al. Circulating Tumor DNA Measurements As Early Outcome Predictors in Diffuse Large B-Cell Lymphoma. J Clin Oncol. 2018;36:2845–53.

37. Eisenhauer EA, Therasse P, Bogaerts J, Schwartz LH, Sargent D, Ford R, et al. New response evaluation criteria in solid tumours: revised RECIST guideline (version 1.1). Eur J Cancer. 2009;45:228–47.

38. Li H, Durbin R. Fast and accurate short read alignment with Burrows-Wheeler transform. Bioinformatics. 2009;25:1754–60.

39. Tarasov A, Vilella AJ, Cuppen E, Nijman IJ, Prins P. Sambamba: fast processing of NGS alignment formats. Bioinformatics. 2015;31:2032–4.

40. Li H, Handsaker B, Wysoker A, Fennell T, Ruan J, Homer N, et al. The Sequence Alignment/Map format and SAMtools. Bioinformatics. 2009;25:2078–9.

41. Ramírez F, Dündar F, Diehl S, Grüning BA, Manke T. deepTools: a flexible platform for exploring deep-sequencing data. Nucleic Acids Res. 2014;42:W187-91.

42. Hellwig S, Nix DA, Gligorich KM, O'Shea JM, Thomas A, Fuertes CL, et al. Automated size selection for short cell-free DNA fragments enriches for circulating tumor DNA and improves error correction during next generation sequencing. PLoS ONE. 2018;13:e0197333.

43. Mouliere F, Chandrananda D, Piskorz AM, Moore EK, Morris J, Ahlborn LB, et al. Enhanced detection of circulating tumor DNA by fragment size analysis. Sci Transl Med. 2018;10.

44. Berger AC, Korkut A, Kanchi RS, Hegde AM, Lenoir W, Liu W, et al. A Comprehensive Pan-Cancer Molecular Study of Gynecologic and Breast Cancers. Cancer Cell. 2018;33:690-705.e9.

45. Chan KCA, Jiang P, Chan CWM, Sun K, Wong J, Hui EP, et al. Noninvasive detection of cancer-associated genome-wide hypomethylation and copy number aberrations by plasma DNA bisulfite sequencing. Proc Natl Acad Sci USA. 2013;110:18761–8.

46. Usadel H, Brabender J, Danenberg KD, Jerónimo C, Harden S, Engles J, et al. Quantitative adenomatous polyposis coli promoter methylation analysis in tumor tissue, serum, and plasma DNA of patients with lung cancer. Cancer Res. 2002;62:371–5.

47. Jensen TJ, Goodman AM, Kato S, Ellison CK, Daniels GA, Kim L, et al. Genome-Wide Sequencing of Cell-Free DNA Identifies Copy-Number Alterations That Can Be Used for Monitoring Response to Immunotherapy in Cancer Patients. Mol Cancer Ther. 2019;18:448–58.